NeuroImage: Clinical 46 (2025) 103772

Contents lists available at ScienceDirect

NeuroImage: Clinical

journal homepage: www.elsevier.com/locate/ynicl

Short-term BCI intervention enhances functional brain connectivity associated with motor performance in chronic stroke

Khosrov A. Grigoryan [a,*], Karsten Mueller [b,c], Matthias Wagner [a], Diaa Masri [a], Kerrin J. Pine [d], Arno Villringer [a,e,f], Bernhard Sehm [a,g]

[a] Department of Neurology, Max Planck Institute for Human Cognitive and Brain Sciences, Leipzig, Germany
[b] Neural Data Science and Statistical Computing, Methods and Development Group, Max Planck Institute for Human Cognitive and Brain Sciences, Leipzig, Germany
[c] Department of Neurology, Charles University, First Faculty of Medicine and General University Hospital, Prague, Czech Republic
[d] Department of Neurophysics, Max Planck Institute for Human Cognitive and Brain Sciences, Leipzig, Germany
[e] Clinic for Cognitive Neurology, University Hospital Leipzig, Leipzig, Germany
[f] Center for Stroke Research, Charité Universitätsmedizin Berlin, Berlin, Germany
[g] Department of Neurology, Martin Luther University of Halle-Wittenberg, Halle, Germany

ARTICLE INFO

Keywords:
Brain-computer interface
Stroke
Functional Connectivity
Resting-state fMRI
Default mode network
Neuroplasticity

ABSTRACT

Background: Evidence suggests that brain-computer interface (BCI)-based rehabilitation strategies show promise in overcoming the limited recovery potential in the chronic phase of stroke. However, the specific mechanisms driving motor function improvements are not fully understood.
Objective: We aimed at elucidating the potential functional brain connectivity changes induced by BCI training in participants with chronic stroke.
Methods: A longitudinal crossover design was employed with two groups of participants over the span of 4 weeks to allow for within-subject (n = 21) and cross-group comparisons. Group 1 (n = 11) underwent a 6-day motor imagery-based BCI training during the second week, whereas Group 2 (n = 10) received the same training during the third week. Before and after each week, both groups underwent resting state functional MRI scans (4 for Group 1 and 5 for Group 2) to establish a baseline and monitor the effects of BCI training.
Results: Following BCI training, an increased functional connectivity was observed between the medial prefrontal cortex of the default mode network (DMN) and motor-related areas, including the premotor cortex, superior parietal cortex, SMA, and precuneus. Moreover, these changes were correlated with the increased motor function as confirmed with upper-extremity Fugl-Meyer assessment scores, measured before and after the training.
Conclusions: Our findings suggest that BCI training can enhance brain connectivity, underlying the observed improvements in motor function. They provide a basis for developing novel rehabilitation approaches using non-invasive brain stimulation for targeting functionally relevant brain regions, thereby augmenting BCI-induced neuroplasticity and enhancing motor recovery.

1. Introduction

Stroke is the leading cause of motor impairment worldwide, and its prevalence is expected to rise as the population ages (Feigin et al., 2021). After treatment-induced and/or spontaneous motor recovery during the acute phase, stroke survivors often reach a functional plateau, following which further recovery is usually slow or stagnant (Grefkes and Fink, 2020). Nevertheless, emerging evidence evinces the potential of motor imagery (MI)-based brain-computer interface (BCI) based rehabilitation therapies in helping individuals surpass the recovery plateau (Cervera et al., 2018; Nojima et al., 2022; Zhang et al., 2024). This plateau underscores the need for innovative approaches that can reignite neuroplastic processes and promote sustained functional improvement.

Traditional rehabilitation methods, including physical and occupational therapy, exhibit limited efficacy in addressing this plateau, particularly for individuals with severe motor deficits. Emerging technologies such as motor imagery (MI)-based brain-computer interfaces (BCIs) offer a promising alternative by leveraging neuroplasticity principles. MI activates cortical regions overlapping with actual movement execution, including the premotor cortex, supplementary motor area

* Corresponding author.
E-mail address: grigoryan@cbs.mpg.de (K.A. Grigoryan).

https://doi.org/10.1016/j.nicl.2025.103772
Received 2 August 2024; Received in revised form 18 March 2025; Accepted 18 March 2025
Available online 19 March 2025

(SMA), and inferior parietal lobule (Donati et al., 2024). However, performing MI without any feedback has drawbacks such as a lack of control over the activity and reduced motivation. BCIs address this limitation by creating closed-loop systems that translate real-time brain activity into visual or somatosensory feedback, actively involving patients in their recovery.

Recent studies advocate for coupling BCI devices with complementary technologies, such as MI-triggered functional electrical stimulation (FES) and incorporating virtual reality for visual feedback (Khokale et al., 2023; Johansson, 2012; Donati et al., 2016). FES delivers precisely timed electrical impulses to peripheral nerves, inducing muscle contractions that mimic natural movement patterns. While early applications focused on gait rehabilitation, modern closed-loop FES systems synchronize stimulation with volitional motor intent, enhancing both functional assistance and plasticity induction (Shin et al., 2022). The transition from open-loop to closed-loop FES systems marked a paradigm shift – EMG-triggered and BCI-controlled FES now enable volitional engagement by linking motor intention to functional movement execution (Shin et al., 2022;Ren et al., 2024). Neuroimaging reveals that MI combined with FES amplifies μ-rhythm suppression in sensorimotor cortices while increasing interhemispheric coherence between primary motor regions (Donati et al., 2024;Yakovlev et al., 2023). This synergy arises through three mechanisms: 1) FES provides congruent somatosensory feedback to enhance MI vividness, 2) peripheral stimulation reinforces central motor commands via thalamocortical loops, and 3) combined MI-FES strengthens cortico-cortical connectivity through Hebbian plasticity (Donati et al., 2024;Ren et al., 2024; Yakovlev et al., 2023).

Modern BCI systems convert MI-related EEG signals into FES-triggered movements, creating a closed sensorimotor loop that simultaneously engages peripheral receptors and central networks (Shin et al., 2022;Ren et al., 2024; Khan et al., 2023). This approach capitalizes on Hebbian plasticity principles – volitional MI paired with contingent FES strengthens cortico-cortical and corticospinal connections through temporal binding of pre- and post-synaptic activity (Ren et al., 2024; Yakovlev et al., 2023). Preliminary evidence suggests such systems induce dual plasticity: 1) local increases in SMN connectivity supporting motor execution, and 2) enhanced DMN-SMN integration facilitating goal-directed attention and error monitoring (Wu et al., 2020).

These findings highlight the potential of combined central-peripheral interventions to drive multifaceted neuroplasticity. However, despite promising hypotheses that strengthening central-peripheral connections through complementary technologies enhances motor recovery via use-dependent plasticity, the precise mechanisms underlying these adaptive brain changes remain poorly characterized.

Resting-state functional MRI has proven to be a powerful tool for investigating functional brain networks in stroke patients, offering insights into changes in functional brain connectivity without the need for task performance, which can be challenging for patients with motor impairments (Fan et al., 2015; Mattos et al., 2023; Cassidy et al., 2021). Unlike task-based functional MRI, which is confounded by task execution, resting-state functional MRI allows characterization of changes associated with recovery and rehabilitation independent of individual performance.

Using resting-state functional MRI, our longitudinal study investigated the effects of a BCI intervention on functional brain connectivity in individuals with stroke, with a specific focus on the default mode network (DMN). The DMN is comprised of interconnected brain regions including the medial frontal gyrus, posterior cingulate cortex, precuneus, and lateral parietal cortex. These regions are significantly more active when the individual is not actively engaged with the external world (Raichle, 2015). Furthermore, there is evidence suggesting that motor skill learning through MI affects the DMN (Ge et al., 2015). It is of particular interest to investigate the DMN in individuals with stroke, as it provides insight into the functional state of the brain unaffected by their clinical or behavioral conditions. Previous studies have demonstrated that lesion location, and time since stroke impact functional connectivity within the DMN, and between the DMN and other networks such as the sensorimotor network (SMN) (Zhang et al., 2016). The DMN also plays an important role in understanding the neural mechanisms of post-stroke cognitive and functional deficits(Li et al., 2022; Sharp et al., 2011; Jiang et al., 2018; Chen et al., 2019), suggesting that changes in the DMN may reflect pathophysiological properties of functional networks. Furthermore, the interaction between the DMN and SMN may facilitate post-stroke motor recovery (Wu et al., 2020). And yet it remains unclear whether the DMN is malleable to intervention, which would suggest potential restorative functional processes in the brain.

In this study, we aimed to address two key mechanistic questions: Is the DMN in individuals with stroke malleable to a short-term intensive BCI intervention? And are functional brain network changes associated with improvements in motor function?

By conducting a longitudinal analysis using resting-state fMRI, we sought to characterize the plasticity of DMN interactions in response to MI-BCI training and explore their relationship with post-stroke motor recovery. These findings could provide critical insights into the neural mechanisms underlying BCI-facilitated rehabilitation and inform the development of more effective therapeutic strategies tailored to individual patient needs.

2. Methods

2.1. Participant cohort

The study included a cohort of 21 individuals with chronic stroke (5 females; mean age: 60.81 ± 8.66 years; detailed characteristics of the participants are provided in Supplementary Table 1; detailed inclusion and exclusion criteria are provided in the Supplementary Table 2).

2.2. Experimental design

We employed a longitudinal delayed-start crossover design with two groups (the timeline of the study is illustrated in Fig. 1). This design enabled both within-subject and cross-group comparisons, while managing the potential influence of the MRI scanner by alternating the order of interventions and measurements. It ensures a more robust examination of the immediate and sustained effects of BCI training addressing methodological considerations to increase the validity of the results.

The primary difference between the two groups was the scheduling of their BCI training sessions. Specifically, Group 1 received the training during the second week, whereas Group 2 received their training in the third week. To monitor the effects of the training, both groups were subjected to a series of MRI scans before and after their respective training weeks. Each of the MRI scans consisted of structural (multi-parametric mapping and diffusion-weighted imaging), and functional (resting-state and task-based) scans. Consequently, participants in Group 1 underwent a total of four MRI sessions, while those in Group 2 had five.

Throughout the weeks when no intervention was scheduled,

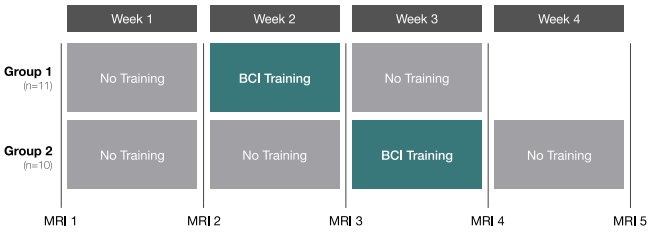

Fig. 1. Experimental Timeline.

participants were asked to continue with their usual daily activities without making any changes that could be attributed to their participation in the study. This is to ensure that any observed effects could be more confidently linked to the BCI training rather than any external factors.

To assess the immediate training effects, the results of BCI training from Group 1′s second week were directly compared with those of Group 2 during the same timeframe. To enhance statistical power and mitigate potential confounding factors, the results of Group 2′s week 3 BCI training were combined with Group 1′s week 2 BCI training outcomes, effectively doubling the sample size for subsequent analyses. Additionally, post-training week outcomes for each group were compared to elucidate sustained effects or variations in performance.

Participants in both groups underwent upper-extremity Fugl-Meyer assessment (UE-FMA) (Fugl-Meyer et al., 1975) before and after their respective BCI-intervention weeks.

All participants have given their written informed consent before participating in the study. The ethical approval for this study was granted by the ethics committee of the Medical Faculty at the University of Leipzig, under the category of fundamental/basic research, with application number 208/17-ek on January 23, 2018.

2.3. Brain-computer interface-based intervention

Participants underwent daily 90-minute BCI training sessions for six consecutive weekdays. The BCI system (recoveriX, g.tec medical engineering GmbH, Schiedlberg, Austria) (Irimia, 2016; Sebastián-Romagosa et al., 2020) was coupled with FES, and virtual avatar. Each session consisted of five trials, interspersed with 5-minute breaks. The trials were used either for classifier training or practice mode. During classifier training trials, the participants received FES and avatar feedback irrespective of whether the system accurately classified their intended movement (left or right wrist dorsiflexion). In contrast, during practice mode trials, feedback was provided only when the system correctly classified the participant's intended movement.

On day 1, four classifier trials were followed by one practice trial. On subsequent days 2–6, one classifier trial was performed to update the classifier, followed by four practice trials.

Before each session, an EEG cap with 16 active electrodes (g.Scarabeo, g.tec medical engineering GmbH, Schiedlberg, Austria) was placed according to the international 10/10 system, with the reference electrode on the right ear, and the ground electrode at FPz.

Individual FES parameters were then adjusted to achieve wrist dorsiflexion. Participants were seated at a table with underarms resting on it. Non-invasive electrodes with adhesive gel were attached to the left and right forearms, targeting the extensor digitorum muscle. The stimulation parameters (frequency, amplitude, phase length) were gradually adjusted until the individual threshold for wrist dorsiflexion was reached.

After the FES parameters were adjusted, the first trial would begin. The participant received an initial auditory warning beep followed two seconds later by a directional arrow ("left" or "right") on the screen. Simultaneously, a corresponding audio command ("left" or "right") was played. In response, the participant was instructed to imagine dorsiflexion of the indicated wrist. If the BCI system detected MI for the instructed side, the system would trigger the FES and virtual avatar feedback. The virtual on-screen avatar mirrored the participant's movement in synchrony with the FES stimulation.

2.4. Magnetic resonance imaging

MRI was performed on a 3 T MAGNETOM Prisma^{fit} (Siemens, Erlangen, Germany) scanner using a 32-channel head coil. High-resolution structural images were acquired using a multi-parametric mapping (MPM) protocol: two multi-echo fast low angle shot (FLASH) scans with T1- and PD-weighting (T1w, PDw), maps of the radio frequency (RF) transmit field $B1^+$ and static magnetic field B0. The MPM acquisition was adapted for whole-brain with a uniform resolution of 1 mm, building upon previously established methods (Weiskopf et al., 2013; Weiskopf et al., 2011; Trampel et al., 2019).

Resting-state fMRI was acquired using a T2*-weighted echo planar imaging (EPI) sequence: axial acquisition orientation, phase encoding A ≫ P, voxel size 2.5 mm isotropic, spacing between slices 2.75 mm, TR 2000 ms, TE 22 ms, flip angle 80°, bandwidth 1795 Hz/pixel, duration 10 min. During each resting-state fMRI scan, participants were instructed to lie still with their eyes open and to loosely fixate a low-contrast crosshair. Before each functional scan, a dual-echo gradient echo non-EPI scan (voxel size 2.5 mm isotropic, TR 620 ms, TE 4 ms, flip angle 60°) and two sets of spin echo EPI scans (voxel size 2.5 mm isotropic, TR 8000 ms, TE 50 ms) were acquired for field map and reverse phase encoding distortion correction, respectively.

All the preprocessing and first-level analysis steps were performed using CONN (Whitfield-Gabrieli and Nieto-Castanon, 2012) (RRID: SCR_009550) release 22.a (Nieto-Castanon and Whitfield-Gabrieli, 2022) toolbox, and second-level analysis was performed using SPM (Penny et al., 2011) (RRID:SCR_007037) release 12.7771.

Preprocessing: Functional and anatomical data were preprocessed using a flexible preprocessing pipeline (Handbook of functional connectivity magnetic resonance imaging methods in CONN, 2020) including creation of voxel-displacement maps, realignment with susceptibility distortion correction using fieldmaps, slice timing correction, outlier detection, indirect segmentation and MNI-space normalization, and smoothing. Functional data were realigned using SPM realign & unwarp procedure (Andersson et al., 2001) integrating gradient echo fieldmaps for susceptibility distortion correction, where all scans were coregistered to a reference image (first scan of the first session) using a least squares approach and a 6 parameter (rigid body) transformation, and resampled using b-spline interpolation (KarlJ et al., 1995) to simultaneously correct for motion, magnetic susceptibility geometric distortions, and their interaction. Temporal misalignment between different slices of the functional data was corrected following SPM slice-timing correction procedure (Sladky et al., 2011), using sinc temporal interpolation to resample each slice fMRI timeseries to a common mid-acquisition time. Potential outlier scans were identified using ART (Whitfield-Gabrieli et al., 2009) as acquisitions with framewise displacement above 0.9 mm or global fMRI signal changes above 5 standard deviations, and a reference image was computed for each subject by averaging all scans excluding outliers. Functional and anatomical data were coregistered and normalized into standard MNI space, segmented into grey matter, white matter, and CSF tissue classes, and resampled to 2 mm isotropic voxels following an indirect normalization procedure using SPM unified segmentation and normalization algorithm (Ashburner and Friston, 2005;Ashburner, 2007) with the default IXI-549 tissue probability map template. Last, functional data were smoothed using spatial convolution with a Gaussian kernel of 8 mm full width at half maximum.

Denoising: In addition to the preprocessing steps, functional data were denoised using CONN's standard denoising pipeline (Handbook of functional connectivity magnetic resonance imaging methods in CONN, 2020) including the regression of potential confounding effects characterized by white matter timeseries (5 CompCor noise components), CSF timeseries (5 CompCor noise components), motion linear and quadratic parameters and their first order derivatives (24 covariates, also known as the Friston-24 model) (Friston et al., 1996), session effects and their first order derivatives (2 covariates), and linear trends (2 covariates) within each functional run, followed by bandpass frequency filtering of the fMRI timeseries (Hallquist et al., 2013) using default cutoff frequencies of 0.008 Hz and 0.09 Hz. CompCor (Behzadi et al., 2007;Chai et al., 2012) noise components within white matter and CSF were estimated by computing the average fMRI signal as well as the largest principal components orthogonal to the signal average, motion parameters within each subject's eroded segmentation masks. From the

number of noise terms included in this denoising strategy, the effective degrees of freedom of the fMRI signal after denoising were estimated to 84.3 across all subjects.

2.5. Seed based analysis

First-level analysis: Seed-based connectivity maps were estimated characterizing the spatial pattern of functional connectivity with a seed area. As we expected functional connectivity alterations within the default-mode network (DMN), seed-based correlation maps were generated for all four regions of the DMN obtained from the HPC-ICA networks (see Supplementary Fig. 1), i.e. four seed-based correlation maps were generated for each participant and each scanning session. Functional connectivity strength was represented by Fisher-transformed bivariate correlation coefficients from a weighted general linear model (weighted-GLM (Handbook of functional connectivity magnetic resonance imaging methods in CONN, 2020), estimated separately for each seed area and target voxel, modeling the association between their fMRI signals. To compensate for possible transient magnetization effects at the beginning of each run, individual scans were weighted by a step function convolved with an SPM canonical hemodynamic response function and rectified.

Second-level analysis: Individual seed-based correlation maps were then entered into a group analysis using SPM12 with a General Linear Model (GLM (Handbook of functional connectivity magnetic resonance imaging methods in CONN, 2020) implementing a flexible-factorial design. Different models were used to implement a repeated-measurements analysis:

Group analysis ***(i)***: Interaction Between Group and Time.

The first group analysis examined two measurements per participant: MRI 2 and MRI 3 (see Supplementary Fig. 2a). A design matrix was constructed to include two factors: GROUP (BCI vs. control) and TIME (pre-intervention vs. post-intervention). Contrast images were generated to test for a potential interaction between these two factors, specifically assessing whether changes over time differed between the BCI and control groups.

2.5.1. Group analysis *(ii)*: effect of intervention across the cohort

The second group analysis aimed to evaluate the overall effect of the intervention across all participants. For this analysis, MRI 2 and MRI 3 were used for Group 1, while MRI 3 and MRI 4 were used for Group 2 (see Supplementary Fig. 2b). The model included a single factor, TIME (pre-intervention vs. post-intervention). Contrast images were generated to identify potential brain connectivity changes associated with the TIME factor by comparing pre- and post-intervention measurements in a paired analysis.

2.5.2. Group analysis *(iii)*: longitudinal analysis across all sessions

The third group analysis investigated pre- and post-intervention differences using a more advanced longitudinal approach to enhance robustness. This model incorporated all available functional sessions: MRI 1, MRI 2, MRI 3, and MRI 4 for Group 1, and MRI 2, MRI 3, MRI 4, and MRI 5 for Group 2 (see Supplementary Fig. 2c). Each participant contributed four input maps, with the model implementing the TIME factor. Contrast images were generated to explore brain connectivity changes associated with the TIME factor across all sessions.

2.5.3. Group analysis *(iv)*: brain connectivity and outcome relationship

The final group analysis assessed the relationship between brain connectivity changes and individual outcomes as measured by the Fugl-Meyer Assessment of Upper Extremity (FMA-UE). To account for the intervention across all participants, MRI 2 and MRI 3 were used for Group 1, while MRI 3 and MRI 4 were used for Group 2 (see Fig. 1). Each participant contributed two input maps, with the model including the TIME factor. Additionally, individual pre- and post-intervention FMA-UE scores were included as covariates (see Supplementary Table 3). This analysis aimed to identify potential correlations between brain connectivity changes and FMA-UE scores.

Note that all analyses were computed at the full-brain level, i.e. parameter estimation was performed for all voxels within the entire brain. Voxel-level hypotheses were evaluated using multivariate parametric statistics with random-effects across subjects and sample covariance estimation across multiple measurements. Inferences were performed at the level of individual clusters (groups of contiguous voxels). Cluster-level inferences were based on parametric statistics from Gaussian Random Field theory (Worsley et al., 1996). Resulting statistical parametric maps were initially assessed using a cluster-forming voxel threshold of $P < 0.005$. To correct for multiple comparisons, significant clusters were obtained with $P < 0.05$ using family-wise error (FWE) correction at the cluster-level (Worsley and Friston, 1995; Eklund et al., 2016; Flandin and Friston, 2019).

2.6. ROI-to-ROI analysis

First-level analysis: ROI-to-ROI connectivity (RRC) matrices were estimated characterizing the functional connectivity between each pair of selected DMN and motor-related regions (DMN networks, precentral gyrus, postcentral gyrus, SMN, SMA) within the CONN Toolbox (Nieto-Castanon and Whitfield-Gabrieli, 2022). Functional connectivity strength was represented by Fisher-transformed bivariate correlation coefficients from a general linear model (weighted-GLM), estimated separately for each pair of ROIs, characterizing the association between their BOLD signal timeseries. In order to compensate for possible transient magnetization effects at the beginning of each run, individual scans were weighted by a step function convolved with an SPM canonical hemodynamic response function and rectified.

Group-level analyses were performed using a General Linear Model (GLM (Handbook of functional connectivity magnetic resonance imaging methods in CONN, 2020). For each individual connection a separate GLM was estimated, with first-level connectivity measures at this connection as dependent variables (one independent sample per subject and one measurement per task or experimental condition, if applicable), and groups or other subject-level identifiers as independent variables. Connection-level hypotheses were evaluated using multivariate parametric statistics with random-effects across subjects and sample covariance estimation across multiple measurements. Inferences were performed at the level of individual clusters (groups of similar connections). Cluster-level inferences were based on parametric statistics within- and between- each pair of networks (Functional Network Connectivity (Jafri et al., 2008), with networks identified using a complete-linkage hierarchical clustering procedure (Sørensen, 1945) based on ROI-to-ROI anatomical proximity and functional similarity metrics. Results were thresholded using a combination of a $p < 0.05$ connection-level threshold and a familywise corrected p-FDR < 0.05 cluster-level threshold (Benjamini and Hochberg, 1995).

2.7. Lesion masking

For each participant, a lesion mask was created by an expert using manual image segmentation. The resulting masks were then verified by a second neurologist for accuracy. For all participants showing a lesion in the right hemisphere ($n = 5$), masks were flipped horizontally (i.e. along the x-axis), resulting in all lesions located uniformly in the left hemisphere (see Fig. 2). All lesion masks were added together, thresholded, and binarized, resulting in a final mask containing an overlay of lesions from all participants. This final mask was added to the statistical analysis as an exclusive mask.

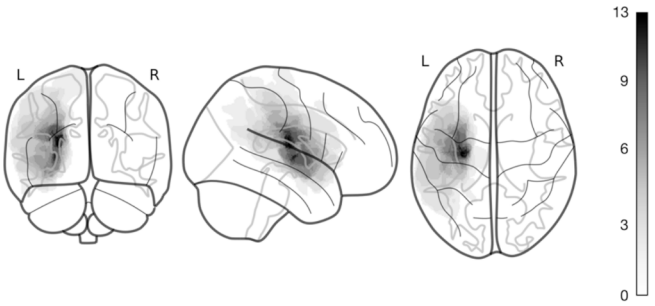

Fig. 2. Cumulative lesion mask. Glass-brain views illustrate the distribution of lesions across all participants. Brighter regions represent areas where fewer participants have lesions, while darker regions represent areas with a higher prevalence of lesions. L – left; R – right.

2.8. Visualization

Figures showing glass-brain images were generated using nilearn (Abraham et al., 2014) (RRID:SCR_001362) v0.10.3 Python library.

Figures showing 3D brain slices were generated using the Mango (Habes et al., 2019) image processing software v4.1 with the statistical parametric maps added as an overlay and were directly obtained from SPM12.

Figures showing ROI-to-ROI connectivity were generated using CONN Toolbox (Nieto-Castanon and Whitfield-Gabrieli, 2022).

3. Results

In the behavioral domain, the 6-day BCI training resulted in improvement in upper limb motor function as assessed by Fugl-Meyer Assessment of Upper Extremity (UE-FMA) scores ($P < 0.0002$, difference in 1.95 scores; see Supplementary Table 3).

To investigate the potential correlation between the motor function improvement and changes in the functional connectivity within the default mode network (DMN), we employed the following models incorporating a repeated-measures design.

Using a two-factorial design with the factors GROUP and TIME (see group analysis ***(i)***), an examination of the interaction between group (BCI vs. control) and time (pre vs. post) showed a differential pattern of pre-post brain connectivity change between the BCI and the control group, with the BCI group exhibiting increased connectivity between the mPFC and left superior parietal gyrus, ipsilesional inferior parietal gyrus, and ipsilesional precuneus (see Fig. 3, and Table 1).

Leveraging the advantage of a crossover design, we pooled intervention weeks from both groups and conducted a pre-post analysis (group analysis ***(ii)***). As anticipated, these results mirrored the findings observed in the interaction analysis, i.e. increase in connectivity between the mPFC and superior and inferior parietal gyri, and precuneus. Additionally, we saw an increase in connectivity between the mPFC and pre-/postcentral gyrus (see Fig. 4, and Table 1).

A pre vs. post analysis of the consolidated corresponding intervention and non-intervention weeks from both groups (group analysis ***(iii)***) reveals significant increase in functional connectivity between mPFC and contralesional SMA, middle cingulate & paracingulate gyri, ipsilesional paracentral lobule, contralesional rolandic operculum, and contralesional pre- and postcentral gyri (see Fig. 5, and Table 1).

When correlating Fugl-Meyer Assessment of Upper Extremity (FMA-UE) scores with the functional connectivity (group analysis ***(iv)***), we observed a significant positive correlation between changes in FMA-UE scores and increased functional connectivity from mPFC to the contralesional pre- and postcentral gyri, ipsilesional superior parietal gyrus, and contralesional precuneus (see Fig. 6, and Table 1).

While seed-based correlation maps were generated for all four regions of the DMN obtained from HPC-ICA networks, significant results were observed only for the mPFC seed region.

In addition to the voxel-wise analyses, a region-of-interest (ROI)-to-ROI connectivity analysis was performed to further explore functional connectivity changes between the medial prefrontal cortex (mPFC) of the default mode network (DMN) and motor-related regions. The analysis revealed significant increases in functional connectivity between the mPFC and several contralesional sensorimotor areas. These included the precentral gyrus (PreCG), which is associated with voluntary motor control and execution, and the postcentral gyrus (PostCG), which is involved in somatosensory processing. Increased connectivity was also observed with the supplementary motor area (SMA), a region critical for motor planning and coordination, as well as with superior and lateral sensorimotor areas, which are linked to the integration of sensory input and motor output (see Fig. 7).

These findings align with and reinforce our seed-based results (group analysis (iii)), providing robust evidence that the intervention enhances functional connectivity between DMN regions and contralesional motor-related areas, further supporting its role in promoting neuroplasticity and motor recovery.

This figure visualizes the results of the ROI-to-ROI analysis. The circular plot at the top illustrates the significant connections between the medial prefrontal cortex (DefaultMode.mPFC) and contralesional sensorimotor regions, including the precentral gyrus (PreCG.r), postcentral gyrus (PostCG.r), supplementary motor area (SMA.r), superior sensorimotor area, and lateral sensorimotor area. The thickness and color intensity of the lines represent the strength of connectivity, with warmer colors indicating stronger positive correlations.

The bottom panel displays 3D renderings of these connections overlaid on brain templates, highlighting their spatial distribution. The red lines represent significant connections.

The table shows the contrast, number of clusters with the number of voxels in the cluster, brain region with T-maximum of the cluster (in bold) and two further local maxima more than 8 mm apart and peak voxel coordinates in MNI space. MNI – Montreal Neurological Institute; x, y, z – coordinates in mm; L – left; R – right.

4. Discussion

In 21 participants with chronic stroke, we show that BCI with MI-triggered functional electrical stimulation (FES) and visual feedback leads to an increased functional connectivity between the mPFC of the DMN and motor-related regions including the premotor cortex, superior parietal cortex, SMA, and precuneus. Additionally, we found increased functional connectivity between the mPFC of the DMN and the superior parietal gyrus. Notably, changes in functional connectivity were positively correlated with improvements in Fugl-Meyer Assessment of Upper Extremity scores.

DMN has been mostly associated with internal modes of cognition (Raichle, 2015), various forms of self-generated thought like episodic memory retrieval, future planning, scene imagination, social cognition, and self-reflection (Andrews-Hanna et al., 2014). Interestingly, DMN connectivity has also been shown to be sculpted by motor learning through altering the interregional connectivity between the medial temporal lobe, lateral temporal cortex, and lateral parietal cortex within the DMN, rather than changing the overall activity of the network (Ge et al., 2015).

Evidence for changes in DMN connectivity after stroke has been reported in several studies. One study in patients with brainstem stroke found a link between DMN connectivity changes and early cognitive dysfunction (Jiang et al., 2018). Furthermore, significantly lower voxel-mirrored homotopic connectivity (VMHC, a technique used to measure the connectivity between mirror areas of the brain hemispheres) in the DMN and motor-related regions was found in subcortical stroke patients, compared to healthy controls, including in the precuneus, parahippocampus, precentral gyrus, supplementary motor area, and middle frontal gyrus (Li et al., 2022). The increased VMHC in the superior

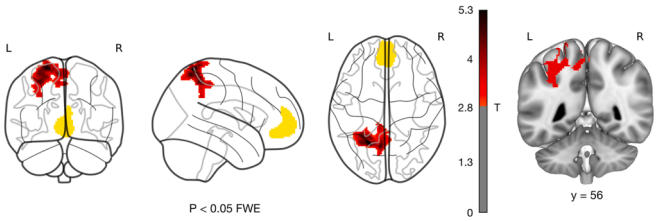

Fig. 3. Glass-brain views and a coronal brain section showing a significant interaction between group (BCI vs. control) and time (pre vs. post). This figure presents the results of a two-factorial analysis examining the interaction between group (BCI vs. control) and time (pre vs. post). The yellow region represents the seed region, located in the medial prefrontal cortex (mPFC) of the default mode network (DMN). The red regions indicate areas with increased functional connectivity with the seed region, specifically in the BCI group compared to the control group: ipsilesional superior parietal gyrus, ipsilesional inferior parietal gyrus, and ipsilesional precuneus. BCI – brain-computer interface; mPFC – medial prefrontal cortex; DMN – default mode network; L – left; R – right. (For interpretation of the references to color in this figure legend, the reader is referred to the web version of this article.)

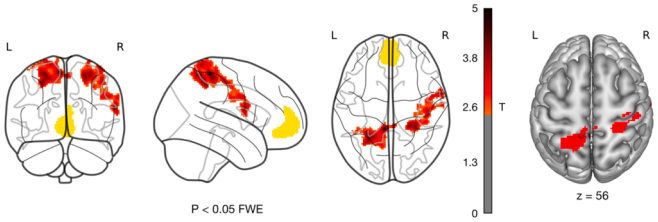

Fig. 4. Glass-brain views and an axial brain section showing significant pre-post-differences. This figure illustrates the results of a pre- versus post-intervention analysis conducted on combined intervention weeks for all participants (n = 42). The yellow region marks the seed region, located in the medial prefrontal cortex (mPFC) of the default mode network (DMN). The red regions represent areas that demonstrated increased functional connectivity with the mPFC following the intervention: superior and inferior parietal gyri, precuneus. mPFC – medial prefrontal cortex; DMN – default mode network; L – left; R – right. (For interpretation of the references to color in this figure legend, the reader is referred to the web version of this article.)

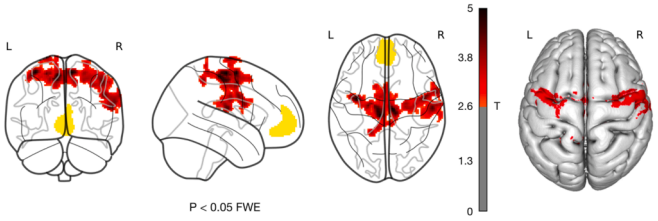

Fig. 5. Glass-brain views and a coronal brain section showing significant pre-post-differences of consolidated intervention and non-intervention weeks. This figure depicts the results of a pre-post analysis of consolidated intervention and non-intervention weeks across both groups (group analysis iii). The yellow region highlights the seed region, located in the medial prefrontal cortex (mPFC) of the default mode network (DMN). The red regions represent areas with significantly increased functional connectivity with the mPFC following the intervention: contralesional SMA, middle cingulate and paracingulate gyri, ipsilesional paracentral lobule, contralesional rolandic operculum, contralesional pre- and postcentral gyri. mPFC – medial prefrontal cortex; DMN – default mode network; L – left; R – right. (For interpretation of the references to color in this figure legend, the reader is referred to the web version of this article.)

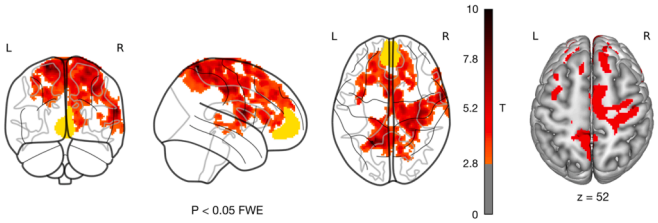

Fig. 6. Glass-brain views and a coronal brain section showing a significant positive correlation of FMA-UE with functional connectivity. This figure illustrates the results of a correlation analysis (group analysis iv) that examined the relationship between Fugl-Meyer Assessment of Upper Extremity (FMA-UE) scores and functional connectivity changes. The yellow region represents the seed region, located in the medial prefrontal cortex (mPFC) of the default mode network (DMN). The red regions indicate areas where increased functional connectivity with the mPFC positively correlated with improvements in FMA-UE scores: contralesional pre- and postcentral gyri, ipsilesional superior parietal gyrus, and contralesional precuneus. mPFC – medial prefrontal cortex; DMN – default mode network; L – left; R – right. (For interpretation of the references to color in this figure legend, the reader is referred to the web version of this article.)

precuneus may reflect functional recovery (Li et al., 2022). Another study investigated functional connectivity changes within the DMN and sensorimotor network in patients with basal ganglia and pontine stroke in the early chronic phase. Compared to healthy controls, patients with basal ganglia stroke exhibited reduced FC in the left precuneus of the posterior DMN (Chen et al., 2019).

Table 1
Summary of brain regions per contrast with significantly increased connectivity with the mPFC of the DMN.

Contrast	Cluster/ extent (n voxels)	Region	Peak voxel coordinates (MNI)			*T* max
			x	y	z	
Interaction between group (BCI vs. control) and time (pre vs. post)	Cluster 1/ 1378					
		Superior parietal gyrus L	**−20**	**−56**	**70**	**5.28**
		Precuneus L	−6	−60	62	4.89
		Inferior parietal gyrus L	−28	−50	52	4.68
Pre vs. post analysis of combined intervention weeks of all participants	Clusters 2/ 1181, 1091					
		Precuneus L	**−6**	**−40**	**62**	**5.85**
		Superior parietal gyrus L	−24	−52	60	4.85
		Inferior parietal gyrus L	−28	−46	50	4.81
		Postcentral gyrus R	**24**	**−36**	**58**	**4.72**
		Precentral gyrus R	62	4	20	4.68
		Postcentral gyrus R	32	−36	62	4.65
Pre vs. post analysis of consolidated intervention and non-intervention weeks	Cluster 1/ 4869					
		SMA R	**8**	**−16**	**62**	**5.01**
		Precentral gyrus L	−36	−4	62	4.97
		Paracentral lobule L	−8	−24	58	4.46
Correlation of FMA-UE scores with functional connectivity	Clusters 2/ 8228, 3307					
		Superior parietal gyrus L	**–22**	**−54**	**72**	**10.41**
		Postcentral gyrus R	64	2	16	8.85
		Precuneus L	−10	−54	68	7.98
		SMA L	**−4**	**6**	**76**	**7.40**
		Superior frontal gyrus, L	–22	42	40	6.35
		SMA L	−2	22	60	6.24

The two aforementioned lines of evidence regarding DMN connectivity, i.e., its alterations after stroke, and the changes induced by motor learning, motivated our approach to test in participants with chronic stroke whether DMN connectivity might be malleable to neurofeedback intervention and therefore be a potential mechanism of recovery. Indeed, we were able to confirm this hypothesis. The increased

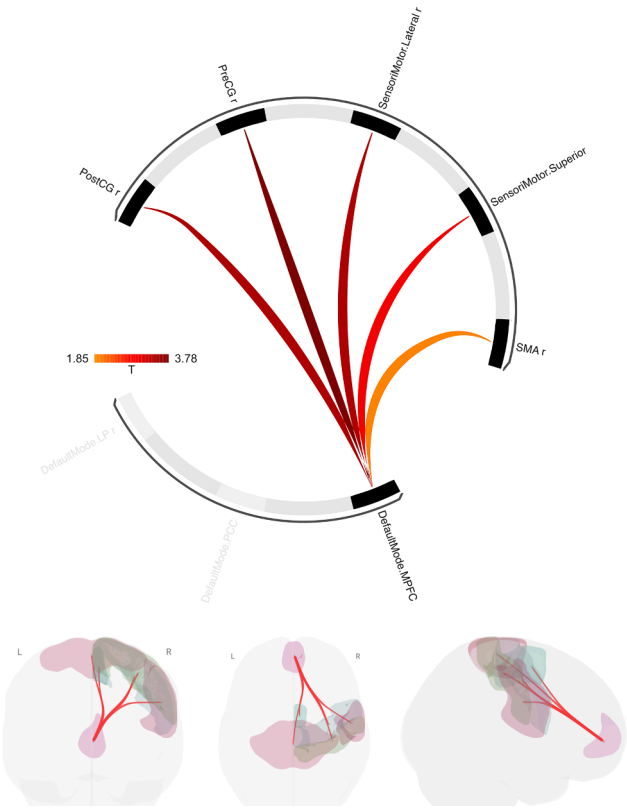

Fig. 7. ROI-to-ROI connectivity analysis showing significant increases in functional connectivity between the mPFC and contralesional sensorimotor regions.

connectivity which we observed between the mPFC and motor regions could reflect the recruitment and integration of cognitive processes facilitated by the DMN in support of motor skill learning and recovery.

In addition to connectivity changes of mPFC to motor-related regions, the BCI group also exhibited increased connectivity between the mPFC and regions such as the ipsilesional superior parietal gyrus, ipsilesional inferior parietal gyrus, and ipsilesional precuneus. The pre-post analysis of consolidated intervention weeks further corroborated and extended these findings, revealing increased functional connectivity between the mPFC and regions such as the SMA, middle cingulate & paracingulate gyri, ipsilesional paracentral lobule, contralesional rolandic operculum, and contralesional pre- and postcentral gyri. The SMA and cingulate cortex are implicated in motor planning and execution (Picard and Strick, 1996), while the paracentral lobule and pre- and postcentral gyri are key components of the primary sensorimotor cortex (Rosazza and Minati, 2011). These connectivity changes suggest that BCI intervention may have facilitated the reorganization and integration of motor control networks, potentially contributing to the observed improvements in upper limb motor function.

Crucially, changes in functional connectivity were positively correlated with improvements in Fugl-Meyer Assessment scores of Upper Extremity. Specifically, increased connectivity from the mPFC to the contralesional pre- and postcentral gyri, ipsilesional superior parietal gyrus, and contralesional precuneus was associated with greater gains in motor skills. These findings provide compelling evidence for the potential neuroanatomical substrates underlying motor skill recovery and highlight the reorganization of interregional communication within the motor network as a key mechanism facilitated by BCI intervention.

The observed connectivity changes around lesioned areas also merit further exploration in the context of perilesional tissue reorganization

post-stroke. Perilesional regions, which border the area of infarct or injury, have been implicated in functional recovery and plasticity mechanisms following stroke (Cramer, 2008). The increased connectivity between the mPFC and regions such as the contralesional pre- and postcentral gyri, ipsilesional superior parietal gyrus, and contralesional precuneus may reflect reorganization within the perilesional tissue, potentially facilitating the recruitment of alternative neural pathways or the unmasking of existing connections. This reorganization could contribute to the observed improvements in motor function by enabling the remapping of motor representations or the formation of new functional networks to compensate for the lesioned areas (Grefkes and Fink, 2014).

The increased connectivity between the mPFC and contralesional regions, such as the superior parietal gyrus and precuneus, invites further consideration in light of emerging perspectives on the contralesional hemisphere's role in stroke recovery. Our findings suggest that the contralesional hemisphere might play a supportive role. The recruitment of areas like the superior parietal gyrus and precuneus could indicate their compensation for the damaged motor cortex in the ipsilesional hemisphere, aligning with the growing recognition of contralesional recruitment in functional recovery, especially during the acute and subacute phases post-stroke (Rehme and Grefkes, 2013).

While this study offers valuable insights into the neural and behavioral effects of BCI intervention, it is not without limitations. The relatively small sample size presents challenges in terms of generalizability and limits the ability to explore more nuanced subgroup analyses. It restricts the ability to detect subtle or complex interactions between variables that could provide deeper mechanistic insights into the observed connectivity changes and motor recovery.

Despite these constraints, several methodological strategies were employed to mitigate their impact. The longitudinal delayed-start crossover design allowed for within-subject comparisons, reducing inter-individual variability and enhancing statistical power. Additionally, combining intervention weeks from both groups effectively doubled the sample size for certain analyses, providing more robust estimates of pre-post intervention effects.

It is also important to note that while this study focused on upper limb motor function recovery, the findings may not be directly generalizable to other motor domains or cognitive functions. Studies with larger and more diverse samples are needed to validate these results across broader populations and explore the applicability of BCI interventions in other domains. Larger cohorts would enable detailed subgroup analyses based on demographic and clinical characteristics, such as age, gender, lesion type, or time since stroke. Such analyses could uncover critical factors influencing individual variability in response to BCI training.

Moreover, multi-center collaborations could facilitate recruitment of larger and more heterogeneous participant pools, enhancing external validity and enabling cross-validation of findings across different populations and settings. These efforts would also allow for exploration of potential additive or synergistic effects when combining BCI interventions with other rehabilitation strategies.

Future studies should explore integrating BCI training with complementary neurostimulation techniques to further enhance recovery outcomes. One particularly promising approach is combining BCI training with non-invasive brain stimulation methods such as transcranial magnetic stimulation (TMS). Applying rTMS to motor-related refions before BCI sessions could potentially create a window of enhanced plasticity, amplifying intervention effects. Similarly, rTMS protocols targeting specific cortical areas might enhance interhemispheric balance or promote connectivity within motor networks, amplifying the effects of BCI-based interventions. Future research should investigate optimal stimulation parameters, timing, and target regions to maximize the synergistic benefits of combining TMS or rTMS with BCI training.

Another promising area is the use of virtual reality (VR) or augmented reality (AR) in combination with BCI. Virtual environments can provide immersive and engaging feedback during motor imagery tasks, which may increase patient motivation and adherence to training protocols. For example, VR-based systems could simulate real-world tasks or gamified scenarios that align with the patient's rehabilitation goals, thereby creating a more meaningful and rewarding training experience. Similarly, AR could overlay visual cues or real-time feedback onto the physical environment, allowing patients to interact with augmented representations of their movements. This could enhance action observation mechanisms, which are known to support motor learning.

Moreover, extended reality (XR) technologies could be used to create closed-loop systems where neural signals detected by the BCI are translated into dynamic visual feedback within the virtual or augmented environment. Such systems could reinforce neuroplasticity by providing immediate and contextually relevant feedback on motor imagery performance. Future studies should investigate how different types of XR feedback—such as first-person versus third-person perspectives or varying levels of task complexity—affect brain connectivity changes and motor recovery outcomes.

Longitudinal studies are also needed to evaluate the long-term sustainability of neural and behavioral changes induced by BCI interventions. Such studies could track participants over months or years to determine whether gains in motor function persist. Imaging-based investigations could provide deeper insights into how brain networks reorganize over time in response to sustained training.

Finally, personalized approaches represent another critical avenue for improving outcomes. Identifying biomarkers that predict individual responsiveness to BCI training—such as lesion characteristics, baseline functional connectivity patterns, or genetic predispositions—could help tailor interventions to each patient's unique needs. This precision-medicine approach would optimize therapeutic efficacy by targeting specific neural pathways or adjusting training intensity based on individual capacity for neuroplasticity.

In summary, our study underscores the efficacy of BCI intervention in fostering motor function recovery through reorganization of brain connectivity patterns and integration of cognitive processes facilitated by the default mode network. The observed neural changes, particularly increased functional connectivity between the medial prefrontal cortex (mPFC) and motor-related regions, highlight a potential neuroanatomical substrate for motor skill recovery and emphasize the significance of interregional communication within the motor network. By addressing current limitations and pursuing these future research directions—such as combining BCI with neurostimulation techniques like TMS, incorporating virtual or augmented reality in the training paradigm, conducting longitudinal studies, expanding applications to other domains, and personalizing interventions—BCI-based rehabilitation strategies can be further optimized for clinical use, ultimately broadening their impact on stroke recovery and neurorehabilitation.

Declaration of Generative AI and AI-assisted technologies in the writing process

During the preparation of this work the authors used Anthropic's Claude 3 Opus in order to improve the readability and the overall language quality of the manuscript. After using this tool, the authors reviewed and edited the content as needed and take full responsibility for the content of the published article.

CRediT authorship contribution statement

Khosrov A. Grigoryan: Writing - review & editing, Conceptualization, Project Administration, Data curation, Visualization, Methodology, Investigation, Formal analysis. **Karsten Mueller:** Writing – review & editing, Visualization, Methodology, Formal analysis. **Matthias Wagner:** Writing – review & editing, Data curation. **Diaa Masri:** Writing –

review & editing, Data curation. **Kerrin J. Pine:** Writing – review & editing, Methodology. **Arno Villringer:** Writing – review & editing, Supervision, Resources, Project administration, Methodology, Investigation, Formal analysis, Conceptualization. **Bernhard Sehm:** Writing – review & editing, Supervision, Methodology, Investigation, Conceptualization.

Funding

This work was supported by the Max Planck Society.

Declaration of competing interest

The authors declare that they have no known competing financial interests or personal relationships that could have appeared to influence the work reported in this paper.

Appendix A. Supplementary data

Supplementary data to this article can be found online at https://doi.org/10.1016/j.nicl.2025.103772.

Data availability

Publicly sharing the raw data is not permissible within the terms of the data protection policies and the ethics approval granted for this study. Derived data that support the findings presented in this study can be obtained by contacting the corresponding author with a reasonable request.

References

Feigin, V.L., Brainin, M., Norrving, B., et al., 2021. World stroke organization (WSO): global stroke fact sheet 2022. *Int J Stroke*. 17 (1), 18–29. https://doi.org/10.1177/17474930211065917.

Grefkes, C., Fink, G.R., 2020. Recovery from stroke: current concepts and future perspectives. *Neurol Res Pr*. 2 (1), 17. https://doi.org/10.1186/s42466-020-00060-6.

Cervera, M.A., Soekadar, S.R., Ushiba, J., et al., 2018. Brain-computer interfaces for post-stroke motor rehabilitation: a meta-analysis. *Ann Clin Transl Neurol*. 5 (5), 651–663. https://doi.org/10.1002/acn3.544.

Nojima, I., Sugata, H., Takeuchi, H., Mima, T., 2022. Brain–computer interface training based on brain activity can induce motor recovery in patients with stroke: a meta-analysis. *Neurorehabilit Neural Repair*. 36 (2), 83–96. https://doi.org/10.1177/15459683211062895.

Zhang, M., Zhu, F., Jia, F., et al., 2024. Efficacy of brain-computer interfaces on upper extremity motor function rehabilitation after stroke: A systematic review and meta-analysis. *NeuroRehabilitation*. 54 (2), 199–212. https://doi.org/10.3233/nre-230215.

Donati, D., Farì, G., Giorgi, F., et al., 2024. Efficacy of motor imagery in the rehabilitation of stroke patients: a scope review. *OBM Neurobiol*. 08 (03), 1–14. https://doi.org/10.21926/obm.neurobiol.2403236.

Khokale, R., Mathew, G.S., Ahmed, S., et al., 2023. Virtual and augmented reality in post-stroke rehabilitation: a narrative review. *Cureus*. 15 (4), e37559. https://doi.org/10.7759/cureus.37559.

Johansson, B.B., 2012. Multisensory stimulation in stroke rehabilitation. *Front Hum Neurosci*. 6, 60. https://doi.org/10.3389/fnhum.2012.00060.

Donati, A.R.C., Shokur, S., Morya, E., et al., 2016. Long-term training with a brain-machine interface-based gait protocol induces partial neurological recovery in paraplegic patients. *Sci Rep*. 6 (1), 30383. https://doi.org/10.1038/srep30383.

Shin, H.E., Kim, M., Lee, D., et al., 2022. Therapeutic effects of functional electrical stimulation on physical performance and muscle strength in post-stroke older adults: a review. *J Korean Geriatr Soc*. 26 (1), 16–24. https://doi.org/10.4235/agmr.22.0006.

Ren, C., Li, X., Gao, Q., et al., 2024. The effect of brain-computer interface controlled functional electrical stimulation training on rehabilitation of upper limb after stroke: a systematic review and meta-analysis. *Front Hum Neurosci*. 18, 1438095. https://doi.org/10.3389/fnhum.2024.1438095.

Yakovlev, L., Syrov, N., Kaplan, A., 2023. Investigating the influence of functional electrical stimulation on motor imagery related μ-rhythm suppression. *Front Neurosci*. 17, 1202951. https://doi.org/10.3389/fnins.2023.1202951.

Khan, M.A., Fares, H., Ghayvat, H., et al., 2023. A systematic review on functional electrical stimulation based rehabilitation systems for upper limb post-stroke recovery. *Front Neurol*. 14, 1272992. https://doi.org/10.3389/fneur.2023.1272992.

Wu, C.W., Lin, S.H.N., Hsu, L.M., et al., 2020. Synchrony between default-mode and sensorimotor networks facilitates motor function in stroke rehabilitation: a pilot fMRI study. *Front Neurosci*. 14, 548. https://doi.org/10.3389/fnins.2020.00548.

Fan, Y.T., Wu, C.y., Liu, H.L., Lin, K.C., Wai, Y.Y., Chen, Y.L., 2015. Neuroplastic changes in resting-state functional connectivity after stroke rehabilitation. *Front Hum Neurosci* 9 (546). https://doi.org/10.3389/fnhum.2015.00546.

Mattos, D.J.S., Rutlin, J., Hong, X., Zinn, K., Shimony, J.S., Carter, A.R., 2023. The role of extra-motor networks in upper limb motor performance post-stroke. *Neuroscience*. 514, 1–13. https://doi.org/10.1016/j.neuroscience:2023.01.033.

Cassidy, J.M., Mark, J.I., Cramer, S.C., 2021. Functional connectivity drives stroke recovery: shifting the paradigm from correlation to causation. *Brain*. 145 (4), 1211–1228. https://doi.org/10.1093/brain/awab469.

Raichle, M.E., 2015. The brain's default mode network. *Annu Rev Neurosci*. 38 (1), 433–447. https://doi.org/10.1146/annurev-neuro-071013-014030.

Ge, R., Zhang, H., Yao, L., Long, Z., 2015. Motor imagery learning induced changes in functional connectivity of the default mode network. *IEEE Trans Neural Syst Rehabilitation Eng*. 23 (1), 138–148. https://doi.org/10.1109/tnsre.2014.2332353.

Zhang, Y., Liu, H., Wang, L., et al., 2016. Relationship between functional connectivity and motor function assessment in stroke patients with hemiplegia: a resting-state functional MRI study. *Neuroradiology*. 58 (5), 503–511. https://doi.org/10.1007/s00234-016-1646-5.

Li, Y., Yu, Z., Zhou, X., Wu, P., Chen, J., 2022. Aberrant interhemispheric functional reciprocities of the default mode network and motor network in subcortical ischemic stroke patients with motor impairment: A longitudinal study. *Front Neurol*. 13, 996621. https://doi.org/10.3389/fneur.2022.996621.

Sharp, D.J., Beckmann, C.F., Greenwood, R., et al., 2011. Default mode network functional and structural connectivity after traumatic brain injury. *Brain*. 134 (8), 2233–2247. https://doi.org/10.1093/brain/awr175.

Jiang, L., Geng, W., Chen, H., et al., 2018. Decreased functional connectivity within the default-mode network in acute brainstem ischemic stroke. *Eur J Radiol*. 105, 221–226. https://doi.org/10.1016/j.ejrad.2018.06.018.

Chen, H., Shi, M., Zhang, H., et al., 2019. Different patterns of functional connectivity alterations within the default-mode network and sensorimotor network in basal ganglia and pontine stroke. *Méd Sci Monit : Int Méd J Exp Clin Res*. 25, 9585–9593. https://doi.org/10.12659/msm.918185.

Fugl-Meyer, A., Jääskö, L., Leyman, I., Olsson, S., Steglind, S., 1975. The post-stroke hemiplegic patient. 1. a method for evaluation of physical performance. *J Rehabilitation Med*. 7 (1), 13–31. https://doi.org/10.2340/1650197771331.

Irimia D, Sabathiel N, Ortner R, et al. RecoveriX: A New BCI-Based Technology for Persons with Stroke1*Research supported by the SME Phase II Instrument recoveriX (No. 693928), the European Union FP7 Integrated Project VERE (No. 257695), and the Romanian Executive Agency for Higher Education, Research, Development and Innovation Funding (UEFISCDI grant PCCA 180/2012). *2016 38th Annu Int Conf IEEE Eng Med Biol Soc (EMBC)*. 2016;2016:1504-1507. doi:10.1109/embc.2016.7590995.

Sebastián-Romagosa, M., Cho, W., Ortner, R., et al., 2020. Brain computer interface treatment for motor rehabilitation of upper extremity of stroke patients—a feasibility study. *Front Neurosci*. 14, 591435. https://doi.org/10.3389/fnins.2020.591435.

Weiskopf, N., Suckling, J., Williams, G., et al., 2013. Quantitative multi-parameter mapping of R1, PD*, MT, and R2* at 3T: a multi-center validation. *Front Neurosci*. 7, 95. https://doi.org/10.3389/fnins.2013.00095.

Weiskopf, N., Lutti, A., Helms, G., Novak, M., Ashburner, J., Hutton, C., 2011. Unified segmentation based correction of R1 brain maps for RF transmit field inhomogeneities (UNICORT). *NeuroImage*. 54 (3), 2116–2124. https://doi.org/10.1016/j.neuroimage.2010.10.023.

Trampel, R., Bazin, P.L., Pine, K., Weiskopf, N., 2019. In-vivo magnetic resonance imaging (MRI) of laminae in the human cortex. *NeuroImage*. 197, 707–715. https://doi.org/10.1016/j.neuroimage.2017.09.037.

Whitfield-Gabrieli, S., Nieto-Castanon, A., 2012. Conn: a functional connectivity toolbox for correlated and anticorrelated brain networks. *Brain Connect*. 2 (3), 125–141. https://doi.org/10.1089/brain.2012.0073.

Nieto-Castanon, A., Whitfield-Gabrieli, S., 2022. *CONN Functional Connectivity Toolbox: RRID SCR_009550, Release 22*. Hilbert Press.

Penny, W.D., Friston, K.J., Ashburner, J.T., Kiebel, S.J., Nichols, T.E., 2011. *Statistical Parametric Mapping: The Analysis of Functional Brain Images*. Elsevier.

Handbook of functional connectivity Magnetic Resonance Imaging methods in CONN. In: *Handbook of Functional Connectivity Magnetic Resonance Imaging Methods in CONN*. Hilbert Press.; 2020:3-16. doi:10.56441/hilbertpress.2207.6598.

Andersson, J.L.R., Hutton, C., Ashburner, J., Turner, R., Friston, K., 2001. Modeling Geometric Deformations in EPI Time Series. *NeuroImage*. 13 (5), 903–919. https://doi.org/10.1006/nimg.2001.0746.

KarlJ, F., Ashburner, J., Frith, C.D., Poline, J.-B., Heather, J.D., Frackowiak, R.S.J., 1995. Spatial registration and normalization of images. *Hum Brain Mapp*. 3 (3), 165–189. https://doi.org/10.1002/hbm.460030303.

Sladky, R., Friston, K.J., Tröstl, J., Cunnington, R., Moser, E., Windischberger, C., 2011. Slice-timing effects and their correction in functional MRI. *NeuroImage*. 58 (2), 588–594. https://doi.org/10.1016/j.neuroimage.2011.06.078.

Whitfield-Gabrieli, S., Nieto-Castanon, A., Artifact, G.S., 2009. *Detection Tools (ART)*.

Ashburner, J., Friston, K.J., 2005. Unified segmentation. *NeuroImage*. 26 (3), 839–851. https://doi.org/10.1016/j.neuroimage.2005.02.018.

Ashburner, J., 2007. A fast diffeomorphic image registration algorithm. *NeuroImage*. 38 (1), 95–113. https://doi.org/10.1016/j.neuroimage.2007.07.007.

Handbook of functional connectivity Magnetic Resonance Imaging methods in CONN. In: *Handbook of Functional Connectivity Magnetic Resonance Imaging Methods in CONN*. Hilbert Press.; 2020:17-25. doi:10.56441/hilbertpress.2207.6598.

Friston, K.J., Williams, S., Howard, R., Frackowiak, R.S.J., Turner, R., 1996. Movement-Related effects in fMRI time-series. *Magn Reson Med*. 35 (3), 346–355. https://doi.org/10.1002/mrm.1910350312.

Hallquist, M.N., Hwang, K., Luna, B., 2013. The nuisance of nuisance regression: Spectral misspecification in a common approach to resting-state fMRI preprocessing reintroduces noise and obscures functional connectivity. *NeuroImage*. 82, 208–225. https://doi.org/10.1016/j.neuroimage.2013.05.116.

Behzadi, Y., Restom, K., Liau, J., Liu, T.T., 2007. A component based noise correction method (CompCor) for BOLD and perfusion based fMRI. *NeuroImage*. 37 (1), 90–101. https://doi.org/10.1016/j.neuroimage.2007.04.042.

Chai, X.J., Castañón, A.N., Öngür, D., Whitfield-Gabrieli, S., 2012. Anticorrelations in resting state networks without global signal regression. *NeuroImage*. 59 (2), 1420–1428. https://doi.org/10.1016/j.neuroimage.2011.08.048.

Handbook of functional connectivity Magnetic Resonance Imaging methods in CONN. In: *Handbook of Functional Connectivity Magnetic Resonance Imaging Methods in CONN*. Hilbert Press.; 2020:26-62. doi:10.56441/hilbertpress.2207.6598.

Handbook of functional connectivity Magnetic Resonance Imaging methods in CONN. In: *Handbook of Functional Connectivity Magnetic Resonance Imaging Methods in CONN*. Hilbert Press.; 2020:63-82. doi:10.56441/hilbertpress.2207.6598.

Worsley, K.J., Marrett, S., Neelin, P., Vandal, A.C., Friston, K.J., Evans, A.C., 1996. A unified statistical approach for determining significant signals in images of cerebral activation. *Hum Brain Mapp*. 4 (1), 58–73. https://doi.org/10.1002/(sici)1097-0193(1996)4:1<58::aid-hbm4>3.0.co;2-o.

Worsley, K.J., Friston, K.J., 1995. Analysis of fMRI time-series revisited—again. *NeuroImage*. 2 (3), 173–181. https://doi.org/10.1006/nimg.1995.1023.

Eklund, A., Nichols, T.E., Knutsson, H., 2016. Cluster failure: Why fMRI inferences for spatial extent have inflated false-positive rates. *Proc Natl Acad Sci*. 113 (28), 7900–7905. https://doi.org/10.1073/pnas.1602413113.

Flandin, G., Friston, K.J., 2019. Analysis of family-wise error rates in statistical parametric mapping using random field theory. *Hum Brain Mapp*. 40 (7), 2052–2054. https://doi.org/10.1002/hbm.23839.

Jafri, M.J., Pearlson, G.D., Stevens, M., Calhoun, V.D., 2008. A method for functional network connectivity among spatially independent resting-state components in schizophrenia. *NeuroImage* 39 (4), 1666–1681. https://doi.org/10.1016/j.neuroimage.2007.11.001.

Sørensen, T., 1945. *A Method of Establishing Groups of Equal Amplitude in Plant Sociology Based on Similarity of Species Content and Its Application to Analyses of the Vegetation on Danish Commons*. Munksgaard https://books.google.de/books?id=rpS8GAAACAAJ.

Benjamini, Y., Hochberg, Y., 1995. Controlling the false discovery rate: a practical and powerful approach to multiple testing. *J R Stat Soc: Ser B (methodol)*. 57 (1), 289–300. https://doi.org/10.1111/j.2517-6161.1995.tb02031.x.

Abraham, A., Pedregosa, F., Eickenberg, M., et al., 2014. Machine learning for neuroimaging with scikit-learn. *Front Neuroinformatics*. 8, 14. https://doi.org/10.3389/fninf.2014.00014.

Habes M, Lancaster JL, Martinez MJ. *Multi-Image Analysis GUI (Mango, Version 4.1)*.; 2019. https://mangoviewer.com/index.html.

Andrews-Hanna, J.R., Smallwood, J., Spreng, R.N., 2014. The default network and self-generated thought: component processes, dynamic control, and clinical relevance. *Ann N York Acad Sci*. 1316 (1), 29–52. https://doi.org/10.1111/nyas.12360.

Picard, N., Strick, P.L., 1996. Motor areas of the medial wall: a review of their location and functional activation. *Cereb Cortex*. 6 (3), 342–353. https://doi.org/10.1093/cercor/6.3.342.

Rosazza, C., Minati, L., 2011. Resting-state brain networks: literature review and clinical applications. *Neurol Sci*. 32 (5), 773–785. https://doi.org/10.1007/s10072-011-0636-y.

Cramer, S.C., 2008. Repairing the human brain after stroke: I. Mechanisms of spontaneous recovery. *Ann Neurol*. 63 (3), 272–287. https://doi.org/10.1002/ana.21393.

Grefkes, C., Fink, G.R., 2014. Connectivity-based approaches in stroke and recovery of function. *Lancet Neurol*. 13 (2), 206–216. https://doi.org/10.1016/s1474-4422(13)70264-3.

Rehme, A.K., Grefkes, C., 2013. Cerebral network disorders after stroke: evidence from imaging-based connectivity analyses of active and resting brain states in humans. *J Physiol*. 591 (1), 17–31. https://doi.org/10.1113/jphysiol.2012.243469.